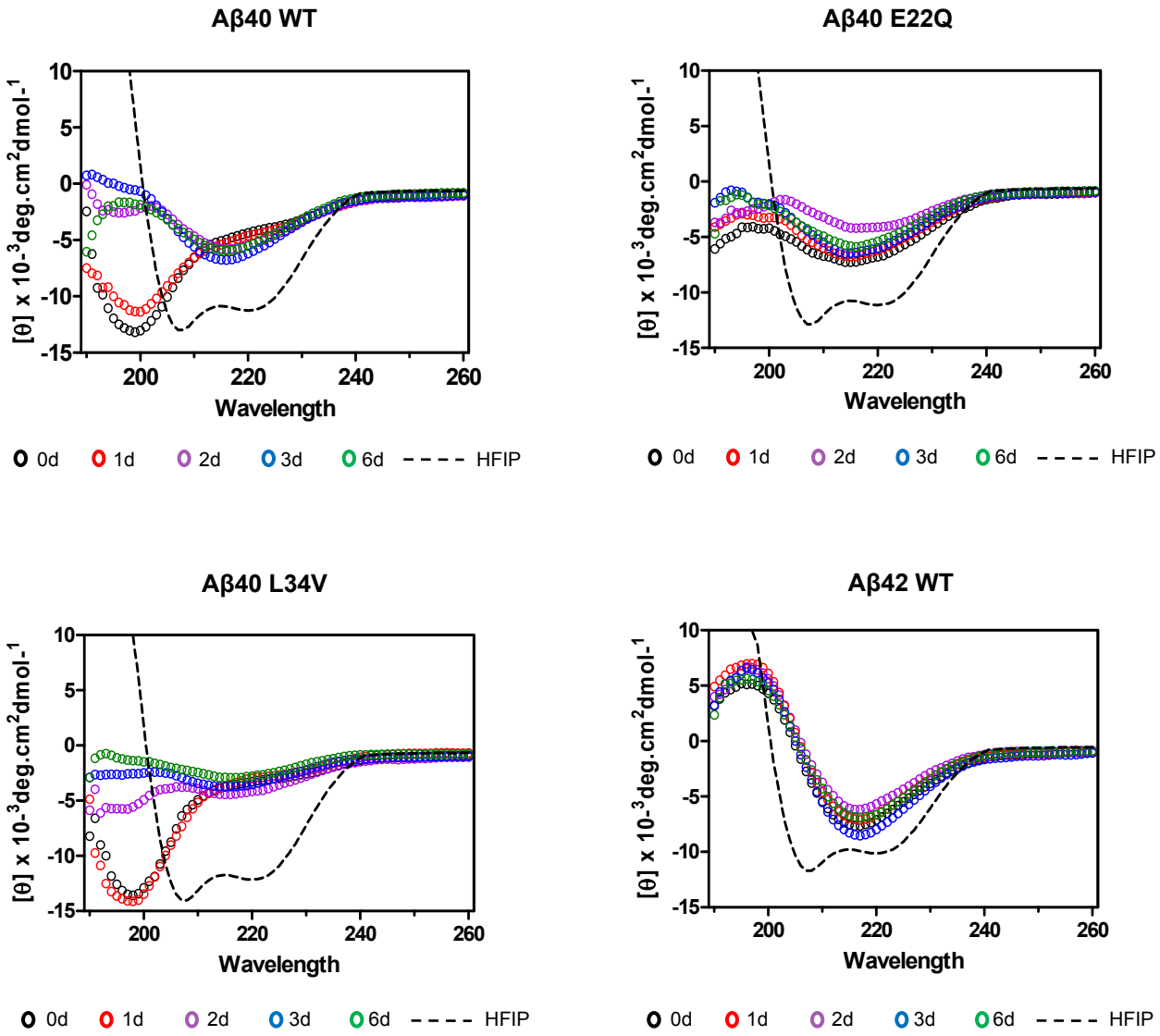

Supplementary Figure 1

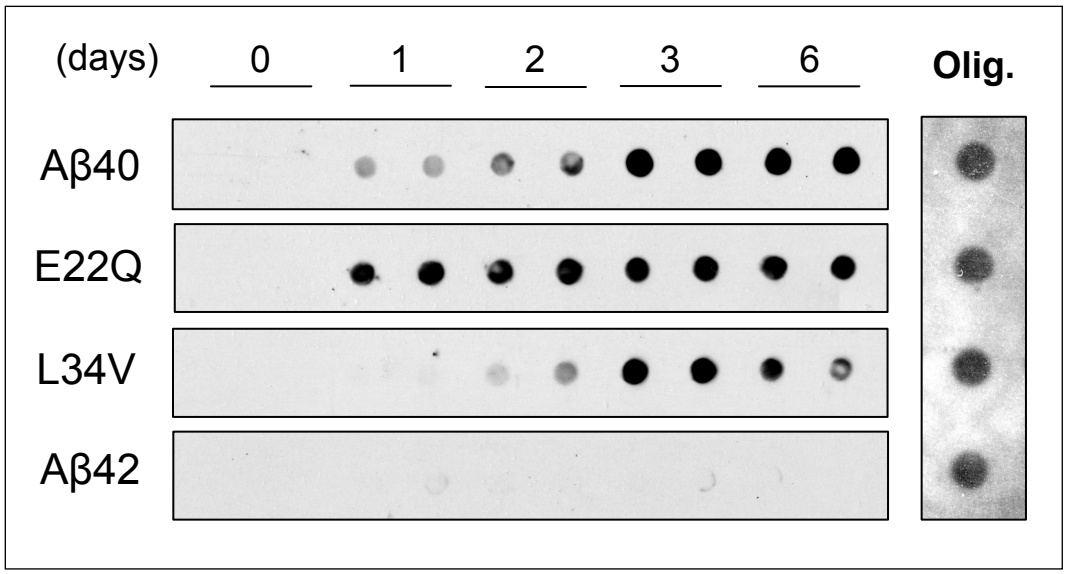

Supplementary Figure 2

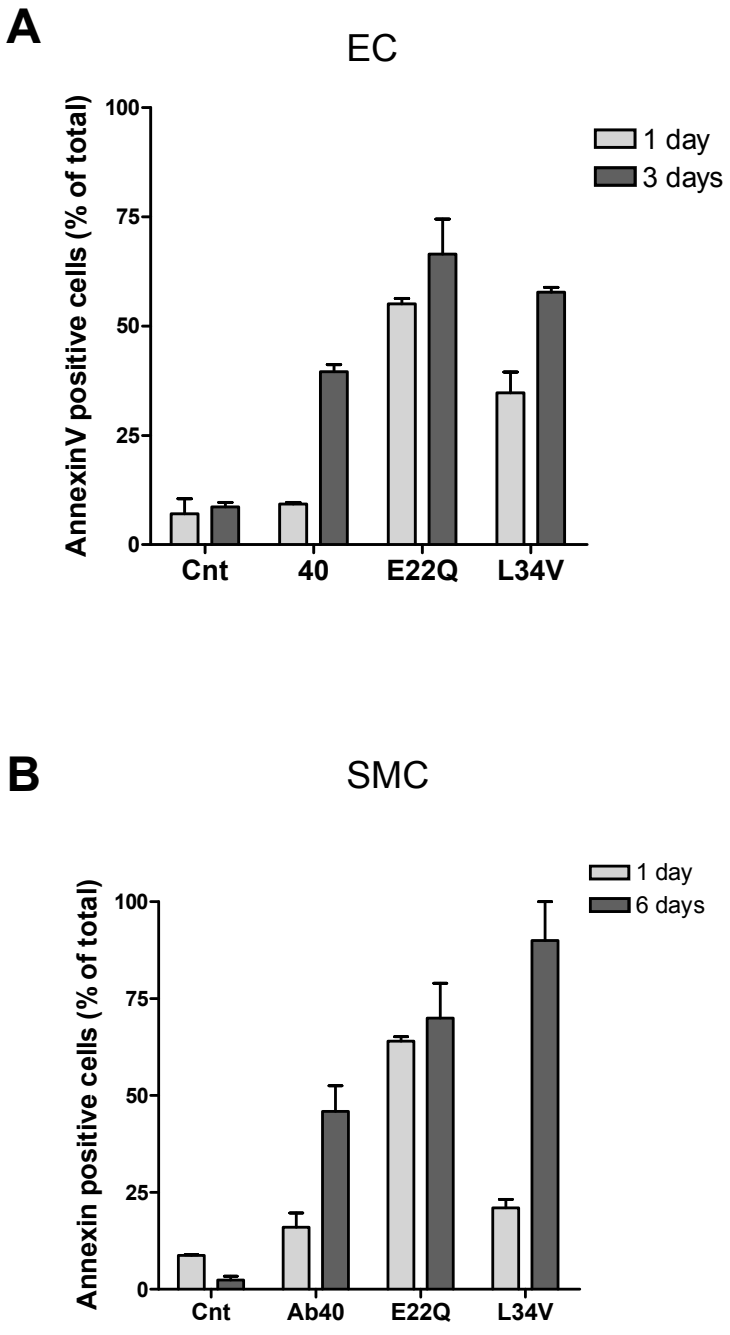

Supplementary Figure 3

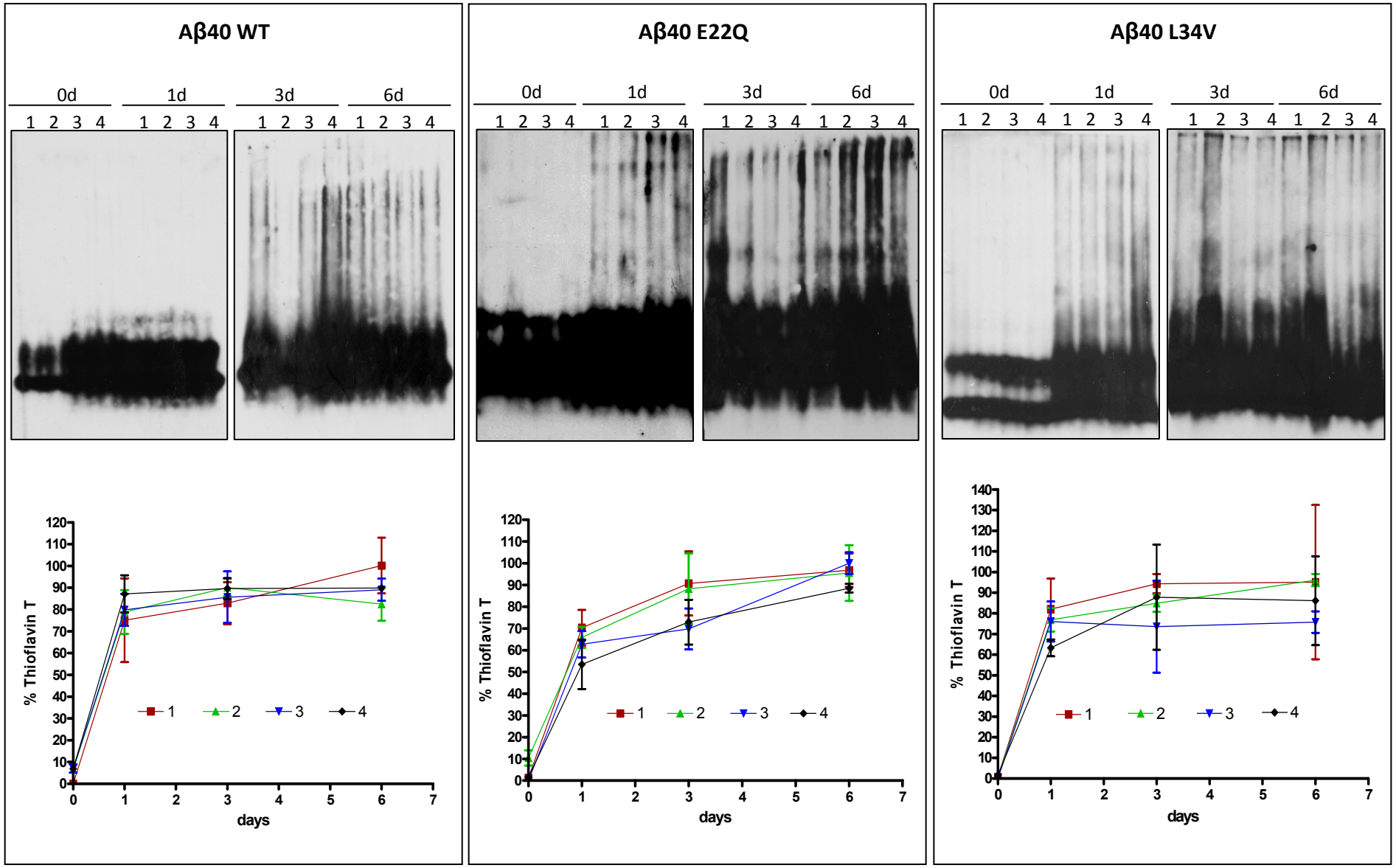

Supplementary Figure 4

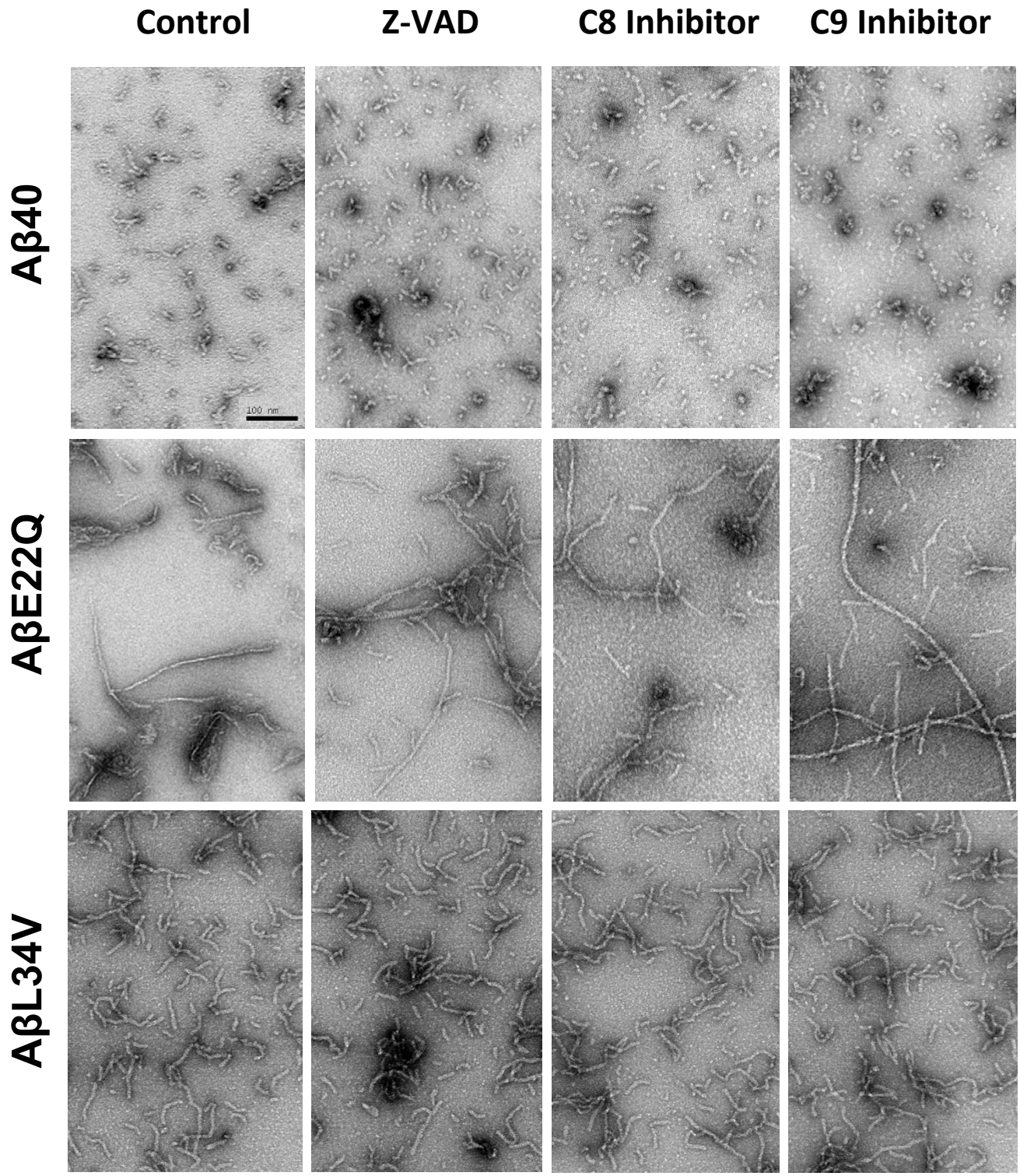

Supplementary Figure 5

SUPPLEMENTARY FIGURE LEGENDS

Supplementary Figure 1: Circular Dichroism (CD). Secondary structure analysis by CD spectroscopy illustrates the different structural characteristics of the peptides. CD spectroscopy of the different amyloid peptides was performed immediately after pre-treatment with HFIP (dashed black line), as well as after reconstitution in PBS and incubation at 37°C from 0 to 6 days. Data represent means of 15 scans after the subtraction of background readings of buffer blanks. In all cases, the spectra after HFIP treatment exhibited the double minimum at 208 and 222 nm characteristic of α-helical structures, indicating that the pretreatment had successfully disrupted β-sheet components with potential seeding capability and generated monodisperse preparations which were subsequently employed as starting points for the aggregation experiments. Wild type-Aβ40 adopted a typical unordered conformation under physiologic salt concentration exhibiting a minimum at 198 nm, a conformation that remained unchanged for up to 1 day. After 2-day incubation, a β-sheet component became evident as indicated by the presence of the typical minimum at 218 nm while still exhibiting some random-coil structural components, as illustrated by the still predominantly negative values below 200 nm. This type of secondary structure remained basically unchanged for the remaining 6-day duration of the aggregation experiments. The highly fibrillogenic Aβ42, as expected, displayed a very distinct β-sheet profile at every time point including immediately after reconstitution in PBS. The genetic variants studied herein revealed a different behavior. While L34V practically did not differ from the wt-Aβ40 peptide, E22Q exhibited an intermediate structural configuration between the latter and Aβ42, in agreement with the data illustrated by native electrophoresis and WB analysis. The CD spectra demonstrated the existence of mixed components, containing β-sheet assemblies

even immediately after solubilization but without achieving the predominant β-sheet conformation of the Aβ42 in the time frame of the experiments.

Supplementary Figure 2: Dot Blot analysis. The formation of oligomeric assemblies during the aggregation experiments was evaluated by Dot blot analysis using A11 anti-oligomer antibody as described in Methods. This conformational antibody is known to recognize soluble oligomeric intermediates failing to immunoreact with both, low molecular weight oligomers as well as with Aβ fibrillar specie. Each time point samples from the aggregation experiments (800 ng) were loaded in duplicate in adjacent wells. Right panel illustrates the A11 immunoreactivity of control wells loaded with 500 ng of the purified SEC-oligomer peak (Sephadex G75).

In agreement with the Thioflavin T-binding and WB data, E22Q aggregated aggressively with strong oligomer formation even at day one. L34V yielded similar results to wt Aβ40 with faint signals for intermediate-size oligomers appearing after 1- and 2-day incubation, and reaching the highest point at day 3. Aβ42, exhibiting preferential formation of fibrillar components as indicated by the highest thioflavin-T fluorescence, showed no immunoreactivity for A11 likely indicating a concentration of these assemblies, under the current experimental conditions, below the sensitivity of the assay, even at short incubation times. The presence of low levels of intermediate oligomers in Aβ42 was confirmed by the positive signal with A11 in 1- and 3-day aggregation samples after purification of the oligomer peak by SEC following centrifugation to separate fibrillar components, as described in methods.

Supplementary Figure 3: Scoring of Annexin V positive cells. A) EC treated with wt-Aβ40, E22Q, and L34V (50μM); **B)** SMC treated with the different Aβ variants. For both (A) and (B),

results are expressed as percent of Annexin V positive cells vs. total number of cells per field; for each experiment two different fields at x200 magnification were counted. Data are representative of three independent experiments. Both, the time frame and the relative capability of the different peptides to induce apoptosis evaluated by Annexin V fluorescence, was comparable to the evaluation by ELISA. L34V emerged as a potent pro-apoptotic inducer for vessel wall cells, comparable in its effect to the highly active E22Q, albeit exhibiting a delayed response, likely reflecting the extended aggregation lag-phase. At 3- and 6-day treatment of EC and SMC respectively, the Piedmont variant induced Annexin V-positive membrane alterations in 60% and 80% of the total cells, respectively. These values were in the same order of those resulting from E22Q challenge (~ 70% Annexin positive cells for both EC and SMC).

Supplementary Figure 4: Comparative study of structural properties of Aβ genetic variants in the presence of caspase inhibitors. HIFP-treated peptides at 1 mg/ml in PBS, prepared as described in Methods, were incubated at 37^{o}Cfor up to 6 days in the presence and absence of caspase inhibitors at a 100 μM concentration and their aggregation/fibrillization propensity analyzed by native gel electrophoresis and Thioflavin-T binding. ***Top Panels***: WB analysis subsequent to non-denaturing electrophoresis in 10-30% gradient polyacrylamide gels. After transfer, nitrocellulose membranes were probed with a mixture of 4G8 and 6E10 antibodies, as in Figure 1. ***Bottom Panels***: Thioflavin-T binding assay of the samples collected at the different time points. Results are expressed in percentage of the maximum fluorescence signal observed for each peptide. In all cases **1:** indicates peptides incubated in the absence of caspase inhibitors; **2:** Aβ peptides incubated with 100 μM Z-VAD; **3:** Aβ peptides aggregated in the presence of

100 µM caspase 8 inhibitor (Z-IETD-FMK); **4:** Aβ variants aggregated in the presence of 100 µM caspase 9 inhibitor (Z-LEHD-FMK).

Supplementary Figure 5: Comparative electron microscopy study of oligomerization/ fibrillization properties of Aβ variants in the presence of caspase inhibitors. Negative staining of the Aβ peptides was performed after 3-days incubation in the presence and absence of caspase inhibitors essentially as described in Methods. The figure illustrates the conformational assemblies of wt-Aβ40, E22Q, and L34V in the absence (Control) or presence of a 100 µM concentration of pan-caspase inhibitor (Z-VAD), caspase 8 inhibitor (Z-IETD-FMK), or caspase 9 inhibitor (Z-LEHD-FMK).